Eur. Phys. J. C (2015) 75:540
DOI 10.1140/epjc/s10052-015-3770-5

THE EUROPEAN PHYSICAL JOURNAL C

CrossMark

Regular Article - Theoretical Physics

Hypocycloidal throat for 2 + 1-dimensional thin-shell wormholes

S. Habib Mazharimousavi[a], **M. Halilsoy**[b]

Department of Physics, Eastern Mediterranean University, Gazimağusa, Turkey

Received: 6 June 2015 / Accepted: 23 October 2015 / Published online: 19 November 2015

Abstract Recently we have shown that for $2+1$-dimensional thin-shell wormholes a non-circular throat may lead to a physical wormhole in the sense that the energy conditions are satisfied. By the same token, herein we consider an angular dependent throat geometry embedded in a $2+1$-dimensional flat spacetime in polar coordinates. It is shown that, remarkably, a generic, natural example of the throat geometry is provided by a hypocycloid. That is, two flat $2+1$ dimensions are glued together along a hypocycloid. The energy required in each hypocycloid increases with the frequency of the roller circle inside the large one.

1 Introduction

Similar to black holes, wormholes in $2+1$ dimensions [1–11] also have a certain degree of simplicity compared to their $3+1$-dimensional counterparts [12]. The absence of gravitational degrees in $2+1$ dimensions enforces us to introduce appropriate sources to keep the wormhole alive against collapse. Instead of general wormholes, our concern will be confined herein to the subject of thin-shell wormholes (TSWs), whose throat is designed to host the entire source [13–17]. From the outset our strategy will be to curve the geometry of the throat and find the corresponding energy-momentum through the Einstein equations on the thin shell [18,19]. Clearly any distortion/warp at the throat gives rise to certain source, but, as the subject is TSWs, the nature of the energy density becomes of the utmost importance. Wormholes in general violate the null-energy condition (NEC) [20–23], which implies also the violation of the remaining energy conditions. The occurrence of negative pressure components in $3+1$ dimensions provides alternatives in the sense that violation of NEC can be accounted for by the pressure, leaving the possibility of an overall positive energy density.

In this paper we choose our throat geometry in the $2+1$-dimensional TSW such that the pressure vanishes, the energy density becomes positive, and as a result all energy conditions are satisfied [18]. This is an advantageous situation in $2+1$ dimensions not encountered in $3+1$-dimensional TSWs. Our method is to consider a hypersurface induced in $2+1$-dimensional flat polar coordinates. Upon determining the energy density it is observed that a natural solution for the underlying geometry of the throat turns out to be a hypocycloid. The standard cycloid is known to be the minimum time curve of a falling particle in a uniform gravitational field which is generated by a fixed point on a circle rolling on a straight line. The hypocycloid on the other hand is generated by a fixed point on a small circle which rolls inside the circumference of a larger circle. The warped geometry of such a curve surprisingly generates an energy density that turns out to be positive. This summarizes in brief, the main contribution of this paper.

In [18] we have constructed a $2+1$-dimensional TSW by considering a flat bulk metric of the form

$$ds^2 = -dt^2 + dr^2 + r^2 d\theta^2 \tag{1}$$

with a throat located at the hypersurface,

$$F(r,\theta) = r - a_0(\theta) = 0. \tag{2}$$

Using the standard formalism of cut and paste technique (see the Appendix) it was shown that the line element of the throat is given by

$$ds_\Sigma^2 = -dt^2 + (a_0^2 + a_0'^2) d\theta^2 \tag{3}$$

with the energy-momentum tensor on the shell

$$S_i^j = \begin{pmatrix} -\sigma_0 & 0 \\ 0 & 0 \end{pmatrix} \tag{4}$$

[a] e-mail: habib.mazhari@emu.edu.tr
[b] e-mail: mustafa.halilsoy@emu.edu.tr

in which

$$\sigma_0 = \frac{1}{4\pi} \frac{\left(a_0'' - a_0 - \frac{2a_0'^2}{a_0}\right)}{\left(a_0'^2 + a_0^2\right)\sqrt{1 + \left(\frac{a_0'}{a_0}\right)^2}}. \tag{5}$$

We note that a prime stands for the differentiation with respect to θ. It was found that with $\sigma_0 \geq 0$ all energy conditions are satisfied, including that the matter which supports the wormhole was physical i.e. not exotic. Finally the total matter contained in the throat can be calculated as

$$U = \int_0^{2\pi} a_0 \sigma_0 \, \mathrm{d}\theta. \tag{6}$$

In the sequel we shall give explicit examples for this integral.

2 The hypocycloid

A hypocycloid [24] is the curve generated by a rolling small circle inside a larger circle. This is a different version of the standard cycloid, which is generated by a circle rolling on a straight line. The parametric equation of a hypocycloid is given by

$$\begin{aligned} x(\zeta) &= (B-b)\cos\zeta + b\cos\left(\frac{B-b}{b}\zeta\right), \\ y(\zeta) &= (B-b)\sin\zeta - b\sin\left(\frac{B-b}{b}\zeta\right) \end{aligned} \tag{7}$$

in which x and y are the Cartesian coordinates on the hypocycloid. B is the radius of the larger circle centered at the origin, $b\,(<B)$ is the radius of the smaller circle, and $\zeta \in [0, 2\pi]$ is a real parameter. Here if one considers $B = mb$, where $m \geq 3$ is a natural number, then the curve is closed and it possesses m singularities/spikes. In Fig. 1 we plot (7) for different values of m with $B = 1$. Let us add that for the particular choice of $B = 1$ and $b = \frac{1}{4}$ the hypocycloid takes the compact form $x = \cos^3\zeta$ and $y = \sin^3\zeta$ with $x^{2/3} + y^{2/3} = 1$. In the following we proceed to determine the form of the energy density σ and the resulting total energy for the individual cases plotted in Fig. 1.

To this end without loss of generality we set $B = 1$ and $b = \frac{1}{m}$ and express σ as a function of ζ. To this aim we parametrize the equation of the throat as

$$\begin{aligned} a &= a(\zeta) = \sqrt{x(\zeta)^2 + y(\zeta)^2} \\ \theta &= \theta(\zeta) = \tan^{-1}\left(\frac{y(\zeta)}{x(\zeta)}\right). \end{aligned} \tag{8}$$

Using the chain rule one finds

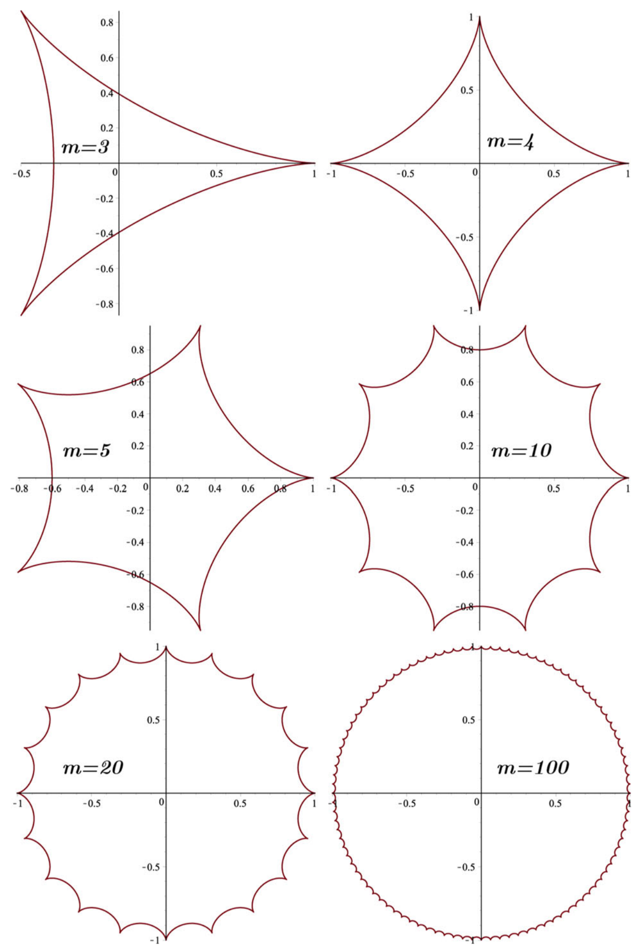

Fig. 1 Hypocycloid for different values of $m = 3, 4, 5, 10, 20, 100$

$$a' = \frac{\mathrm{d}a}{\mathrm{d}\theta} = \frac{\dot{a}}{\dot{\theta}} \tag{9}$$

and

$$a'' = \frac{\mathrm{d}^2 a}{\mathrm{d}\theta^2} = \frac{\ddot{a}\dot{\theta} - \dot{a}\ddot{\theta}}{\dot{\theta}^3}, \tag{10}$$

which implies

$$\sigma = \frac{1}{4\pi} \frac{a\ddot{a}\dot{\theta} - a\dot{a}\ddot{\theta} - a^2\dot{\theta}^3 - 2\dot{\theta}\dot{a}^2}{\left(\dot{a}^2 + a^2\dot{\theta}^2\right)^{\frac{3}{2}}} \tag{11}$$

where a dot stands for the derivative with respect to the parameter ζ. Consequently the total matter is given by

$$U = \int_0^{2\pi} u \, \mathrm{d}\zeta \tag{12}$$

where $u = a\sigma\dot{\theta}$ is the energy density per unit parameter ζ. Note that for the sake of simplicity we dropped the subindex 0 from the quantities calculated at the throat. Particular examples of calculations for the energy U are given as follows.

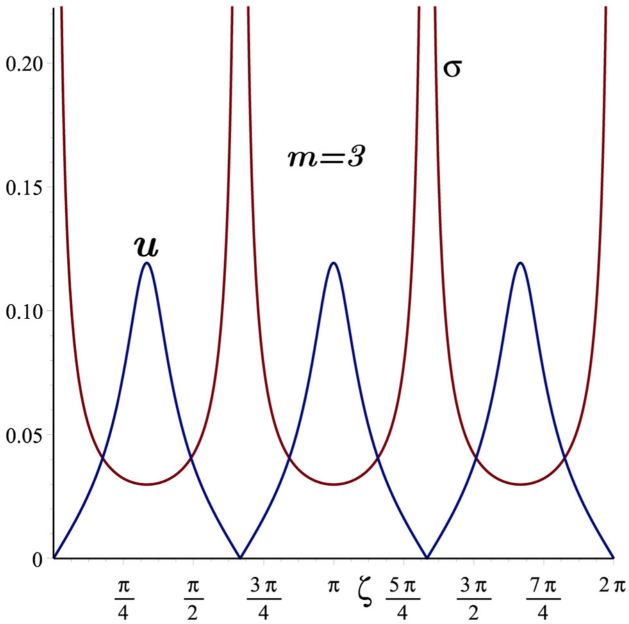

Fig. 2 Plot of σ and u in terms of ζ for $m = 3$. The singularities/cusps of σ are not physical. This can easily be seen when the total energy is finite. This is in analogy with a conical conductor of finite total charge, but the charge density at the vertex diverges

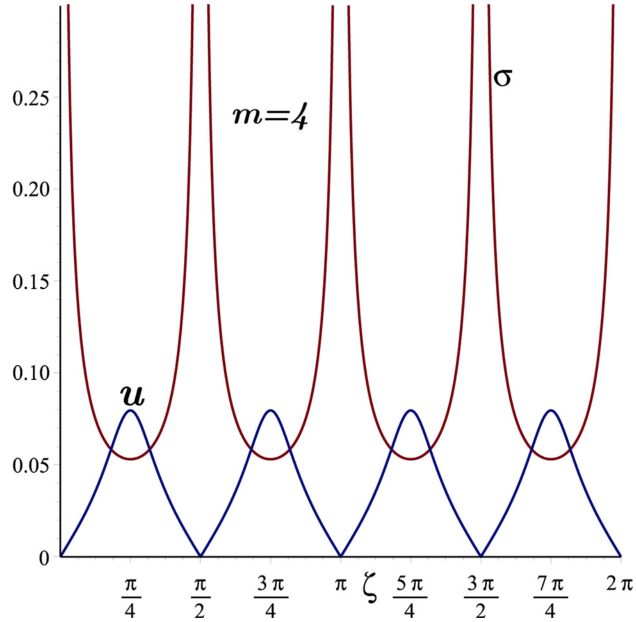

Fig. 3 Plot of σ and u in terms of ζ for $m = 4$. Similar to $m = 3$, the singularities of σ are not physical

2.1 $m = 3$

The first case which we would like to study is the minimum index for m, which is $m = 3$. We find that

$$\sigma = \frac{3\sqrt{2}}{32\pi\sqrt{(1+2\cos\zeta)^2(1-\cos\zeta)}}, \tag{13}$$

which is clearly positive everywhere. Knowing that the period of the curve (7) is 2π we find that σ is singular at the possible roots of the denominator, i.e., $\zeta = 0, \frac{2\pi}{3}, \frac{4\pi}{3}, 2\pi$. We note that although σ diverges at these points the function that must be finite everywhere is u, which is given by

$$u = \frac{3\sqrt{2}\sqrt{(1+2\cos\zeta)^2(1-\cos\zeta)}}{16\pi\sqrt{5-12\cos\zeta+16\cos^3\zeta}}. \tag{14}$$

The situation is in analogy with the charge density of a charged conical conductor whose charge density at the vertex of the cone diverges while the total charge remains finite. In Fig. 2 we plot σ and u as a function of ζ, which clearly implies that u is finite everywhere, leading to the total finite energy $U_3 = 0.099189$.

We would like to add that physically nothing extraordinary happens at the cusp points. These points are the specific points at which the manifold is neither differentiable with respect to r nor with respect to the angular variable θ. The original thin-shell wormhole has been constructed based on discontinuity of the manifold with respect to r at the location of the throat which implied the presence of the matter source at the throat (we refer to Fig. 1 of Ref. [25] where clearly such a cuspy point in the r direction is shown). Now, in the case that we study we have one additional discontinuity of the Riemann tensor in the θ direction which implies a more complicated form of the matter distribution at the throat.

2.2 $m = 4$

Next, we set $m = 4$ where one finds

$$\sigma = \frac{1}{6\pi\sqrt{\sin^2(2\zeta)}} \tag{15}$$

and

$$u = \frac{\sqrt{\sin^2(2\zeta)}}{8\pi\sqrt{1-3\cos^2\zeta+3\cos^4\zeta}}. \tag{16}$$

Figure 3 depicts σ and u in terms of ζ and, similar to $m = 3$, we find $\sigma > 0$ and u finite with the total energy given by $U_4 = 0.24203$. As one observes, $U_4 > U_3$, which implies that adding more cusps to the throat increases the energy needed. This is partly due to the fact that the total length of the hypocycloid is increasing as m increases such that $\ell_m = \frac{8(m-1)}{m}$ with $B = 1$. This pattern goes on with m larger, and in general

$$u = \frac{(m-2)^2\sqrt{(\cos\zeta-\cos(m-1)\zeta)^2}}{8\pi\sqrt{2}\sqrt{\Psi}} \tag{17}$$

Table 1 Total energy U_m in terms of m. We add that the total energy for large m is approximately given by $U_{m\to\text{large}} \approx \frac{m}{2\pi}$. This shows that increasing the number of cusps to infinity requires infinite energy

m	3	4	5	10	50	100
U_m	0.099189	0.24203	0.39341	1.1767	7.5351	15.492

where

$$\Psi = m^2 - 2(m-1)\cos^2(m-1)\zeta - (m-2)^2\cos\zeta\cos(m-1)\zeta - m^2\sin(m-1)\zeta\sin\zeta - 2(m-1)\cos^2\zeta. \qquad (18)$$

Table 1 shows the total energy U_m for various m. We observe that U_m is not bounded from above (with respect to m), which means that for large m it diverges as $U_m \approx \frac{m}{2\pi}$. Therefore to stay in a classically finite energy region one must consider m to be finite.

3 Conclusion

The possibility of a total positive energy has been scrutinized and verified with explicit examples in the $2+1$-dimensional TSWs. Naturally the same subject arises with more stringent conditions in the more realistic dimensions of $3+1$. By taking advantage of the technical simplicity we have shown that, remarkably, the geometry of the throat can be that of a hypocycloid. This is a rare curve compared with the more familiar minimum time cycloid. In effect, a fixed point on the circumference of a smaller circle rolling in a larger one makes a hypocycloid. The important point is that in the rolling process the concavity of the resulting curve makes the extrinsic curvature negative, which in turn yields a positive energy density σ. Note that with convex curves this is not possible. The emerging cusps at the tips of the hypocycloid may yield singular points; however, these can be overcome by integrating around such cusps. The lightning rod analogy for a diverging charge density in electromagnetism constitutes an example to understand the situation. In the present case our sharp points (edges) are reminiscent of cosmic strings and naturally deserve a separate investigation. The result for the total energy turns out to be perfectly positive, as our analytical calculation and numerical plots reveal. Increasing frequency of each roll by using smaller and smaller circles inside the large one is shown to increase the regular energy in finite amounts, which is necessary to give life to a TSW. The fact that in a static frame the pressure vanishes simplifies our task. Here once $\sigma > 0$ is chosen it implies automatically that the energy conditions are also satisfied. Finally, gluing together two curved spaces instead of flats will be our next project to address along the same line of thought.

Funded by SCOAP^3.

Appendix: Extrinsic curvature tensor

The bulk metric is flat given by (1), therefore we cut out $r < a(\theta)$ from the bulk and make two identical copies of the rest manifold. We paste them at the timelike hypersurface $F(r,\theta) = r - a(\theta) = 0$ to construct a complete manifold. The induced metric on the hyperplane Σ is given by (3). The extrinsic curvature tensor on the shell Σ is given by

$$K_{ij}^{(\pm)} = -n_\gamma^{(\pm)}\left(\frac{\partial^2 x^\gamma}{\partial y^i \partial y^j} + \Gamma^\gamma_{\alpha\beta}\frac{\partial x^\alpha}{\partial y^i}\frac{\partial x^\beta}{\partial y^j}\right) \qquad (A1)$$

in which $x^\gamma = (t, r, \theta)$ is the coordinate of the bulk metric and $y^i = (t, \theta)$ is the coordinate of the shell. Also

$$n_\gamma^{(\pm)} = \frac{\pm 1}{\sqrt{\Delta}}\frac{\partial F}{\partial x^\gamma} \qquad (A2)$$

where

$$\Delta = g^{\alpha\beta}\frac{\partial F}{\partial x^\alpha}\frac{\partial F}{\partial x^\beta} \qquad (A3)$$

refers to the normal 3-vector to the shell and $\pm$ implies the different sides of the shell.

The Israel junction [26–30] conditions read

$$-8\pi S_i^j = k_i^j - \delta_i^j k \qquad (A4)$$

in which $S_i^j = \text{diag}(-\sigma, p)$ is the energy-momentum tensor on the shell (we note that the off-diagonal term is zero) and $k_i^j = K_i^{j(+)} - K_i^{j(-)}$ with $k = k_i^i$. The explicit calculation reveals that

$$n_\gamma^{(\pm)} = \pm\frac{a}{\sqrt{a^2 + a'^2}}(0, 1, -a') \qquad (A5)$$

and

$$k_i^j = \begin{bmatrix} 0 & 0 \\ 0 & \frac{2(a^2+2a'^2-aa'')}{(a^2+a'^2)^{3/2}} \end{bmatrix}. \qquad (A6)$$

References

1. M.S. Delgaty, R.B. Mann, Int. J. Mod. Phys. D **4**, 231 (1995)
2. G.P. Perry, R.B. Mann, Gen. Relativ. Gravit. **24**, 305 (1992)
3. S.-W. Kim, H.-J. Lee, S.K. Kim, J. Yang, Phys. Lett. A **183**, 359 (1993)
4. C. Bejarano, E.F. Eiroa, C. Simeone, Eur. Phys. J. C **74**, 3015 (2014)
5. W.T. Kim, J.J. Oh, M.S. Yoon, Phys. Rev. D **70**, 044006 (2004)
6. M. Jamil, M.U. Farooq, Int. J. Theor. Phys. **49**, 835 (2010)
7. V.-L. Saw, L.Y. Chew, Gen. Relativ. Gravit. **44**, 2989 (2012)

8. F. Rahaman, A. Banerjee, I. Radinschi, Int. J. Theor. Phys. **51**, 1680 (2012)
9. K. Skenderis, B.C. van Rees, Commun. Math. Phys. **301**, 583 (2011)
10. S. Aminneborg, I. Bengtsson, D. Brill, S. Holst, P. Peldan, Class. Quantum Gravity **15**, 627 (1998)
11. D. Brill, *in Mathematical and quantum aspects of relativity and cosmology (Pythagoreon, 1998)*, ed. by S. Cotsakis, G.W. Gibbons. Lecture Notes in Physics, vol **537** (Springer, Berlin, 2000), pp. 143–179. arXiv:gr-qc/9904083
12. M.S. Morris, K.S. Thorne, Am. J. Phys. **56**, 395 (1988)
13. M. Visser, Phys. Rev. D **39**, 3182 (1989)
14. M. Visser, Nucl. Phys. B **328**, 203 (1989)
15. P.R. Brady, J. Louko, E. Poisson, Phys. Rev. D **44**, 1891 (1991)
16. E. Poisson, M. Visser, Phys. Rev. D **52**, 7318 (1995)
17. M. Visser, *Lorentzian Wormholes from Einstein to Hawking* (American Institute of Physics, New York, 1995)
18. S.H. Mazharimousavi, M. Halilsoy, Eur. Phys. J. C **75**, 81 (2015)
19. S.H. Mazharimousavi, M. Halilsoy, Eur. Phys. J. C **74**, 3067 (2014)
20. D. Hochberg, M. Visser, Phys. Rev. D **56**, 4745 (1997)
21. C. Barceló, M. Visser, Class. Quantum Gravity **17**, 3843 (2000)
22. D. Ida, S.A. Hayward, Phys. Lett. A **260**, 175 (1999)
23. L.C. Garcia de Andrade, Mod. Phys. Lett. A **15**, 1321 (2000)
24. N.C. Rana, P.S. Joag, *Classical Mechanics* (Tata McGraw-Hill, New Delhi, 2001), pp. 230–232. ISBN 0-07-460315-9
25. S.H. Mazharimousavi, M. Halilsoy, Phys. Rev. D **90**, 087501 (2014)
26. W. Israel, Nuovo Cimento **44B**, 1 (1966)
27. V. de la Cruz, W. Israel, Nuovo Cimento **51A**, 774 (1967)
28. J.E. Chase, Nuovo Cimento **67B**, 136 (1970)
29. S.K. Blau, E.I. Guendelman, A.H. Guth, Phys. Rev. D **35**, 1747 (1987)
30. R. Balbinot, E. Poisson, Phys. Rev. D **41**, 395 (1990)